

PAPER • OPEN ACCESS

## Two-Phase Heat Transfer in 4.0 mm Tube Under Different Gravity Conditions

To cite this article: Giorgia Lancione *et al* 2020 *J. Phys.: Conf. Ser.* **1599** 012009

View the [article online](#) for updates and enhancements.



**ECS** **240th ECS Meeting**  
Digital Meeting, Oct 10-14, 2021  
**We are going fully digital!**  
Attendees register for free!  
**REGISTER NOW**

## Two-Phase Heat Transfer in 4.0 mm Tube Under Different Gravity Conditions

Giorgia LANCIONE<sup>1</sup>, Daiane Miekio ICERI<sup>2</sup>, Luca GUGLIERMETTI<sup>1</sup>, Luca SARACENO<sup>3</sup>, Giuseppe ZUMMO<sup>3\*</sup>, Fabio BISEGNA<sup>1</sup>, Fabio NARDECCHIA<sup>1</sup>

<sup>1</sup> Università di Roma “La Sapienza”, Dipartimento di Ingegneria Astronautica, Elettrica ed Energetica

<sup>2</sup> Heat Transfer Research Group, University of Sao Paulo, Sao Carlos School of Engineering, Department of Mechanical Engineering, Av. Trabalhador Sancarlense, 400, Pq. Arnold Schmidt, Sao Carlos, SP, Brazil

<sup>3</sup> ENEA, via Anguillarese, 301, Rome, Italy

\* Corresponding author e-mail: [giuseppe.zummo@enea.it](mailto:giuseppe.zummo@enea.it)

**Abstract.** This study aimed to analyze the two-phase heat transfer in a vertical upward flow configuration under different gravity conditions. The facility is a new version of MicroBo (Microgravity Boiling), the working fluid used is perfluorohexane C<sub>6</sub>F<sub>14</sub> and a 4.0 mm aluminum channel is arranged vertically to perform ebullition process. The platform used to get data in microgravity was the parabolic flight, which represents one of the most widely used platforms despite the period of time available to collect data is very short. The analysis of the results has been carried out following two main approaches: the first, ground-flight data comparison, for the study of variable gravity data collected during the 67th ESA campaign of parabolic flight held in November 2017, while the second, ground data analysis, to analyze the data collected on the ground in the ENEA laboratory with the same facility in December 2018. In particular ground – flight data have been analyzed comparing boiling curves at different flow rates, from a minimum of 5.3 l/h up to 17 l/h, in micro, hyper and normal gravity. The operating inlet pressure during experiments has been fixed at 1.6 bar with a heat flux range of 5.4 - 85.6 kW/m<sup>2</sup>. For what regard ground data boiling curves, with a flow rate of 10 l/h, are shown with a direct flow pattern visualization. The operating pressure has been fixed at 1.3 bar and 1.8 bar with a heat flux range of 2.5 – 94.6 kW/m<sup>2</sup>. For the latter analysis, it also has been carried out a qualitative study for the validation of the void fraction model, starting from the visualization of the images of flow patterns recorded during the acquisitions.

### 1. Introduction

A study of the Flow Boiling Heat Transfer (FBHT) mechanism at different gravity and in micro-tubes is discussed. FBHT is present in many engineering fields, for terrestrial applications and it is in development for space applications. The efficiency of heat removal due to forced convection boiling has promoted the implementation of two-phase in many thermal management applications where power



loads are sufficiently high to make single-phase counterpart insufficient. In particular, micro-evaporators, thanks to their weight and dimension, are expected to play a vital role in the miniaturization of cooling systems. Therefore, they also have the potential of reducing capital cost and environmental problems such as global warming. Many studies have been carried out on the flow boiling in microchannels under low gravity conditions to well understand the phenomenon for both horizontal and vertical channels, as discussed by Saitoh et al. [1], Luciani et al. [2], Baldassari and Marengo [3]. Fang et al. [4] studied the hypergravity conditions inside 1 and 2 mm tubes. During flow boiling many heat transfer regimes and flow patterns take place and this is due to the increasing vapor quality along the channel. Flow patterns may also change in case of vertical or horizontal tube because of gravity. For this reason, the most used configuration is the vertical up-flow in which the buoyance forces help the mixture flow and enhance the heat transfer increasing the slip velocity between vapor and liquid, due to their different densities. The flow patterns prediction is not yet clear because of the various morphological configurations that a vapor-liquid can acquire, also because there is a dependence on a lot of parameters such as surface tension forces and different density of the two phases. To perform flow boiling tests at different gravity conditions, parabolic flight gravity platform was used, which is one of the most used gravity platforms for these experiments as discussed by Konishi and Mudawar [5]. This because, with respect to other gravity platforms like drop towers and sounding rockets, parabolic flight presents some advantages as the ability to accommodate larger experimental packages, test many different operating conditions in multiple parabolas during the same flight, and grant the experimenter manual access to the facility.

## 2. Experimental set description

In this section the experimental facility will be described. MicroBo (Microgravity Boiling) is an experimental facility specifically developed for studying flow boiling in microgravity conditions with in-flight experiments. The parabolic flight imposes many constrains on the section, the system must be safe and compact. This is the reason of many design choices made despite they are not the most efficient in term of performances and layout.

Experimental loop consists in three main system: the main fluid loop, the air loop and the second confinement.

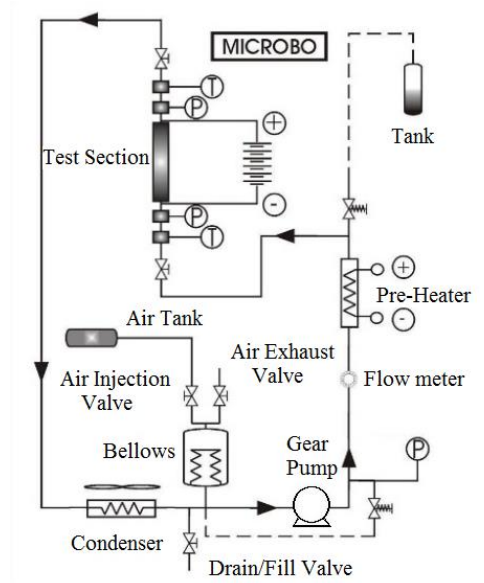


Figure 1: Experimental loop layout

Main components of the main fluid loop are a gear pump, a flowmeter, a preheater, the test section, a condenser and a fluid tank, as can be seen in Figure 1. The fluid used was pure (99.9%) perfluorohexane (C<sub>6</sub>F<sub>14</sub>), a fluorinert liquid which was developed to be used as cooling fluid for electronic components and for boiling systems; it is harmless for people. The test section is made by an aluminum alloy (Aluminum AlSi10Mg) tube that can resist at more than 260°C. The inner tube diameter is 4 mm and the heated length is 150 mm. The channel is heated by Joule effect; a DC electrical supplier, controlled by the operator during experiments, is used to give power to the test section ensuring a uniform heat flux along the channel. The channel is displaced vertically, so that no stratification occurs with respect to axial dimension and it is possible to have symmetry on flow patterns and on wall temperature measurements. The test section is also confined, due to in-flight security constrains, into a special box made of two transparent polycarbonate windows to allow direct inspection. The tube has been thermally insulated to avoid heat losses. Moreover, a transparent tube is placed just at the exit of the heated channel, in the box confinement. The transparent section is used to film the refrigerant flux at the exit with an high-speed camera.

Ten thermocouples have been placed, inserted in specifically designed cavities, along the tube for wall temperature measurement.

**Table 1:** Thermocouples position

<b>THERMOCOUPLES</b>			
	<b>Position 1</b>	<b>Position 2</b>	<b>Position 3</b>
	T1, T2	T3, T4, T5, T6	T7, T8, T9, T10
<b>Axial position from the inlet [m]</b>	0,0151	0,071	0,1311
<b>Axial position from the inlet [%]</b>	10,06	47,33	87,4

The condenser is made by two coaxial copper tubes. The outer tube works as second confinement while the fluid flows into the inner one reducing the total heat transfer of the condenser. In this system, the cooling fluid is air moved by a fan in a forced flow upon the condenser. For safety reasons, the two tubes are placed into a polycarbonate cylinder that isolates the hot surface to avoid any kind of direct contact. The expected  $\Delta T$  in the condenser is 60: the inlet temperature of the fluid in the condenser is about 90 while the outer temperature of the fluid is about 30, to avoid the presence of bubbles at the exit.

Due to the inefficiency of this system, an additional condenser has been added to the loop; a Peltier cell has been placed at the exit of the condenser to cool down it and improve the heat exchange. Once the fluid is cooled and in liquid phase, a gear pump is used to pump the fluid from the outlet of the condenser to the inlet of a filter before entering in the pre-heater. It is used to heat the liquid up to the required test section inlet temperature, reducing subcooling degree. It consists of a flat electrical resistance (75 W, maximum power) covered with silicone rubber and attached on the outer surface of the heat exchanger. Due to parabolic flight constrain, pre-heater is placed quite far from the inlet of test section inducing a heat loss along the tube. Hence, the fluid enters in the test section highly subcooled, 12 - 23 K in this study. Two thermocouples, positioned respectively on the heat exchanger inner wall and on the preheater outlet, allows the operator to control outlet temperature, monitoring the test section inlet temperature and the subcooling degree. A vapor trap, made by two small tanks, is used for degassing the fluid. Non-condensable gases can permeate through the membrane of the tank, therefore the degassing procedure allow to remove these gases before each experiment. A metal pressurized tank is used as the pressure control system. Inside the tank is placed an elastic membrane which divides the fluid and air. Acting on the air pressure, it is possible to regulate the fluid loop pressure. In particular in air loop, air is pumped by the operator into a tank, containing air only, using a mechanical pump every 2 or 3 parabolas. Controlling by software the loading valve and the discharging valve increasing or reducing the occupied volume by the air in the pressurize tank, it is possible to control main loop pressure.

Second confinement loop is realized to contain any accidental fluid leakage from the main loop. It consists in rectangular tanks containing all main components of the main loop, as valves, the filter, sensors and the pre-heater, while pipes are inserted in a corrugated tube. The volume of the second

confinement loop is about three times the volume of the main loop. In particular, BOX 1 is an aluminum box that contains the additional cooler with the Peltier cells. BOX 2 is a rectangular aluminum box in which pre-heater, expansion tanks and valves are placed in. At least, BOX 3, that contains the test section, is made by ERTACEL®, a transparent material which allow flow visualization. The second confinement loop is shown in Figure 1, represented by the green dashed lines.

### 3. Input data uncertainties

The system uncertainties on MicroBo input data are presentend in Table 2. They reach their lower value at maximum heat transfer coefficient ( $\omega h z = 7.9\%$ ). The corresponding uncertainty for thermodynamic quality is higher ( $\omega x z = 27.2\%$ ). Uncertainties and test method used to calculate them are reported in Iceri et al. [6].

**Table 2:** Input parameters uncertainties

UNCERTAINTIES		
Electrical tension	0.1	V
Current	0.01	A
Length	$5 \cdot 10^{-5}$	m
Temperature	0.3	°C
Heat transfer coefficient	$94.01 \cdot 10^{-3}$	w/m <sup>2</sup> K
Pressure in	$6 \cdot 10^{-2}$	bar
Pressure drop	$105 \cdot 10^{-4}$	bar
Mass Flux	$163.66 \cdot 10^{-8}$	kg/s
Vapor quality	0.02	-
Heat flux	1.8	%

### 4. Test procedure

The parabolic flight is one of the gravity platforms used to perform flow boiling tests at different gravity conditions. The time of a parabola is about 1 minute and the procedure can be divided in different phases:

- Regulation starts 60 s before the pull up.
- Data acquisitions starts 50 s before the pull up.
- Checklist, to check all test parameters and experimental loop main components, is performed 45 s before the pull up.
- Parabola starts.

During a parabola, the system is subjected to hyper gravity phases, about 1,8 – 2 g, and to a micro gravity phase of about  $10^{-2}$  g. The problem of data acquired in parabolic flight is related to the fact that available period for acquisition is low, just 20 second for each gravity condition. This means that it is difficult to achieve steady state. This work is developed on the data acquisition performed on the 67th ESA Parabolic Flight campaign in November 2017 and The French company Novespace was appointed to organize the campaign logistics and provide technical supervision of the experiment preparation.

### 5. Tests matrix

Here, a general overview of all tests done in this work is presented. In particular, the most important input parameters, such as mass flux, inlet temperature, inlet pressure and heat flux range, are shown in the Table and it is also reported the information about the gravity level in which the tests were performed.

**Table 3:** Test matrix

Name	Mass Flux	T inlet	P inlet	$\Delta T_{sub}$	Heat flux range	Gravity level		
	kg/m <sup>2</sup> s	°C	bar	°C		1g	0g	2g
TEST 1	117	48	1,6	22	6,5 – 65,6	✓	✓	✓
TEST 2	221	50	1,6	20	9,8 – 75,8	✓	✓	✓

<b>TEST 3</b>	331	50	1,6	20	6,6 – 85,6	✓	✓	✓
<b>TEST 4</b>	375	50	1,6	20	5,4 – 56,1	✓	✓	✓
<b>TEST 5</b>	221	45	1,8	23	2,5 – 94,6	✓	X	X
<b>TEST 6</b>	221	45	1,3	19	7,3 – 64,3	✓	X	X

A parameter of considerable importance for the description of the tests is the degree of subcooling of the fluid at the entrance to the test section. Knowing, in fact, how much the liquid is subcooled, it is possible to better understand the boiling phenomenon that will occur inside the tube.

As can be seen from the TEST 1, TEST 2, TEST 3 and TEST 4 have been performed at different gravity levels by means of parabolic flight platform. In particular, the flight data were collected on the 67th ESA Parabolic Flight in November 2017 while ground data were collected in the ENEA laboratory in November 2017.

On the contrary, TEST 5 and TEST 6 have been carried out only at earth gravity in December 2018 to test MicroBo for high heat flux, near to the thermal crisis zone.

For this reason, two different analysis have been developed in this work:

- GROUND – FLIGHT DATA COMPARISON
- GROUND DATA ANALYSIS

## 6. Results and discussion

As already said, two main approaches to experimental data have been developed: ground- flight data comparison and ground data analysis.

In this paragraph, experimental results are described. In particular boiling curves are presented.

### 6.1. Ground-flight data comparison

Firstly, boiling curves are presented. The wall superheat, on the x-axis, is directly linked with the heat flux, on the y-axis. In this study, the wall superheat is evaluated with respect to the mean wall temperature measured by the thermocouples placed in position 2, shown in section 2.

In the figure 2 are also reported the flow patterns obtained for each experimental point plotted on the curve so that it is possible to well understand the process.

In particular:

- BF = bubbly flow
- BF/SF = bubbly flow to slug flow transition
- SF = slug flow
- SF/AF = slug flow to annular flow transition
- AF = annular flow

As can be seen, boiling starts in subcooled regime with a negative  $\Delta T_{sat}$ . The fluid enters with a certain subcooled degree and boiling starts in partial developed zone. As the thermal flux increases, the wall temperature reaches a certain superheat degree, where saturated boiling starts. Film boiling region occurs for high thermal fluxes where annular flow pattern is visible. Here, heat transfer is strongly enhanced; the curve tends to become vertical which means that the wall superheat increases very slightly as the thermal flux increases.

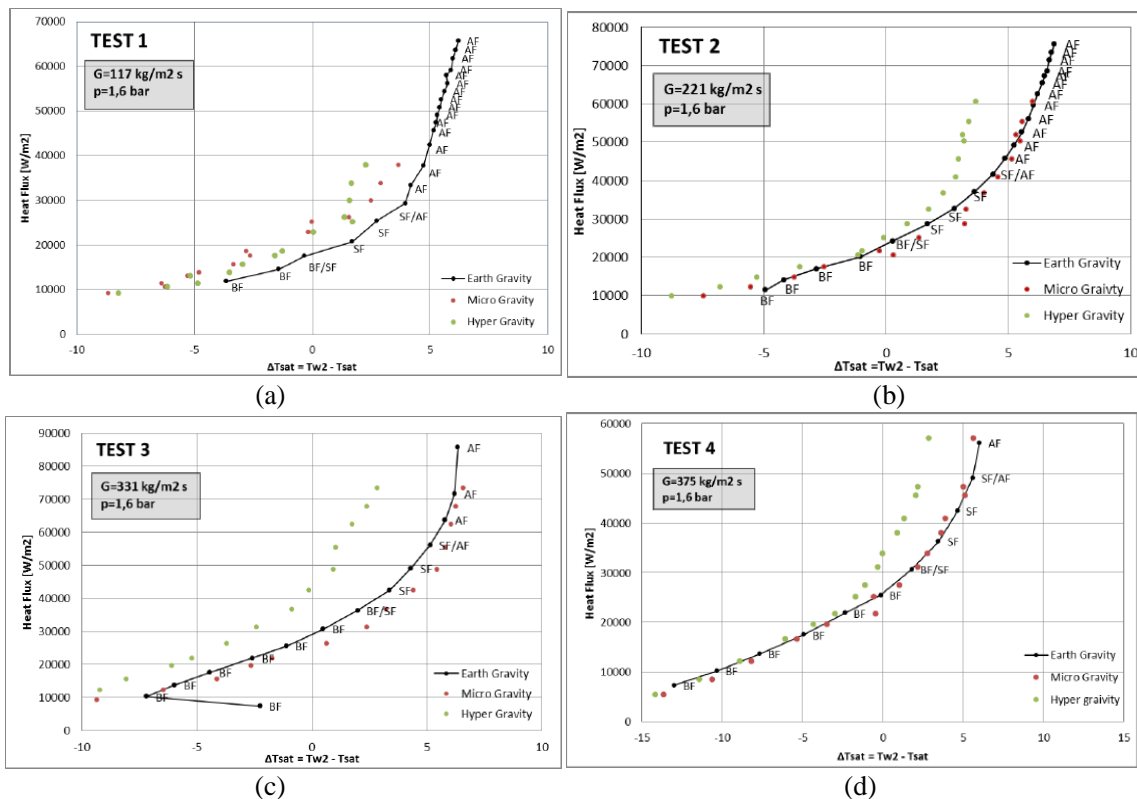


**Figure 2:** (a) Boiling curve TEST 1 in normal, micro and hyper gravity; (b) Boiling curve TEST 2 in normal, micro and hyper gravity; (c) Boiling curve TEST 3 in normal, micro and hyper gravity; (d) Boiling curve TEST 4 in normal, micro and hyper gravity

No substantial differences could be noticed for micro gravity compared with normal gravity especially for high mass flux, while it seems to be not true for hyper gravity. This is related to the fact that during parabolic flight, no steady conditions have been reached in hyper gravity level. It could be also noted, from boiling curves, that the heat transfer seems to be enhanced in hyper gravity conditions; the curve is on the left side of the figures 2a, 2b, 2c, 2d, which means lower wall superheat degree needed for the same heat flux value. This could depend on the induced turbulences that in microgravity are not present because there is no relative velocity between vapor and liquid which, instead, influences boiling mechanism at normal and, especially, hyper gravity.

In all of these tests, fluid enters in the test section with a certain degree of subcooling. Heat fluxes at which the saturated boiling occurs are between  $20.000 \text{ W/m}^2$  and  $30.000 \text{ W/m}^2$  for TEST 2,3 and 4 while for TEST 1, at a lower flow rate, saturate boiling occurs between  $15.000 \text{ W/m}^2$  and  $20.000 \text{ W/m}^2$ . It also important to notice that no single-phase data have been acquired. Only in TEST 3, ONB point is reported just for earth gravity condition.

### 6.2. Ground data analysis

It is reported the boiling curve of TEST 5 and TEST 6 with the images of the flow pattern recorded during the experiments. TEST 5 was performed at  $221 \text{ kg/m}^2 \text{ s}$  mass flux (10 l/h) at a pressure of about 1,8 bar while TEST 6 was performed at  $221 \text{ kg/m}^2 \text{ s}$  mass flux (10 l/h), as TEST 5, but with a lower system pressure of about 1,3 bar.

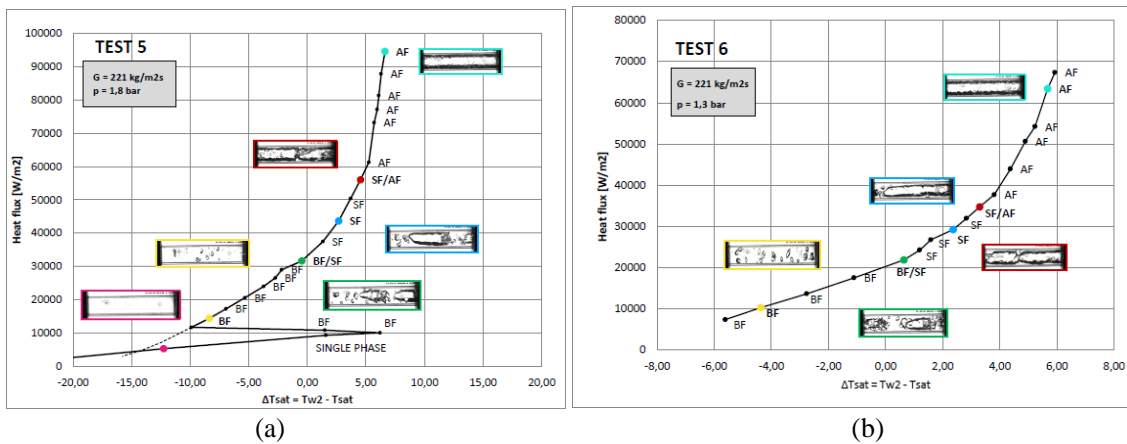


**Figure 3:** (a) Boiling curve TEST 5 with direct flow pattern visualization; (b) Boiling curve TEST 6 with direct flow pattern visualization

Firstly analyzing TEST 5, the liquid enters the test section subcooled,  $\Delta T_{sub}$  of about 23, and boiling is subcooled up to a heat flux of about 30.000 W/m<sup>2</sup>. Then, saturated boiling starts up to 94.588 W/m<sup>2</sup>. Fluid begins to boil with a  $\Delta T$  between the wall temperature and the saturation temperature of about 6 C, where the wall temperature taken into account is the one measured by the thermocouples located at the half of the heated length. To check the exact point of ONB it was necessary to make some measurements starting from low heat fluxes and increasing it little by little, until transition from bubbly to slug flow occurs. The ONB (Onset of Nucleate Boiling), is represented by the peak to the right which is located at low fluxes, about 10.000 W/m<sup>2</sup>. As can be seen, it is the point in which the transition from liquid single-phase to bubbly flow occurs.

Analyzing TEST 6, the fluid at inlet of test section is highly subcooled,  $\Delta T_{sub}$  of about 19, and boiling is subcooled up to a heat flux of about 20.000 W/m<sup>2</sup>. Then, saturated boiling starts. Comparing the result with TEST 5, it can be noted that the heat flux value at which onset of saturated boiling occurs is lower in TEST 6. This is due to the operative pressure, that influences saturation temperature, which is lower than TEST 5 one. Contrary to the TEST 5, no acquisition was made in a single liquid phase in TEST6 because it was not possible to keep the pressure constant at the fixed value. This is the reason why data refer directly to the bubbly flow.

However, it must be specified that the transition between a flow pattern to another is not well defined with world agreement but depends on the observation of the author as discussed by Thome and Cheng [7]. For this reason, it more correct to refer at a transition region and not to a transition point, as also fixed in the boiling curve. The following images represent a qualitative visualization of the flow patterns. They refer to increasing heat fluxes, starting from the single-phase liquid up to the annular flow.

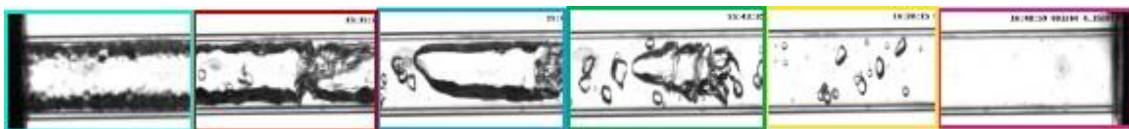


**Figure 4:** Qualitative visualization of flow patterns of TEST 5

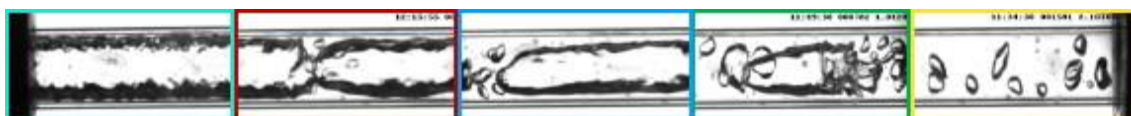


**Figure 5:** Qualitative visualization of flow patterns of TEST 6



The two transition regions are reported in the images with red and green frame. The green one shows the transition from bubbly flow to slug flow while in the red one it is reported slug to annular transition. By focusing attention on the annular flow, in TEST 5 it is possible to notice that the thickness of the liquid film, measured by visual inspection, is thin (the ratio between liquid film thickness measure from image and tube radius is of 0,31). This means that the system is close to the thermal crisis even if it has not been reached.

In TEST 6, it is even clearer from the images, the thin layer of liquid present in the annular flow. It is also possible to observe that the turbulence at the liquid-vapor interface is also reduced with respect to TEST 5. From this it can be inferred that for the maximum heat fluxes, the system was very close to the thermal crisis. Comparing the maximum heat fluxes reached in TEST 5 and TEST 6, it is possible to notice that the values are different. In particular, in TEST 5 the value is around  $90.000 \text{ W/m}^2$  while in TEST 6 is about  $70.000 \text{ W/m}^2$ . This underlines the problem of the definition of flow pattern. They cannot be strictly related to the thermal flux because they depend on many operating parameters such as pressure and saturation temperature.

## 7. Conclusions

This paper aimed to study the two-phase heat transfer in a small channel under normal and micro gravity conditions on MicroBo facility. In particular, boiling curves and flow patterns analysis have been proposed. Key observations from this study can be summarized as follow.

- There is no substantial difference on heat transfer process between normal gravity and low gravity conditions for high mass flux.
- In hyper gravity conditions, heat transfer seems to be enhanced with respect to normal gravity conditions. In these tests, with the heat fluxes applied to the test section, flow patterns in hypergravity are dominated by bubbly and slug flow. With these two flow patterns, images show larger relative vapor velocities compared to normal and micro- gravity conditions. Therefore, larger turbulence at the bubble tails are expected and as consequence the convective component of the heat transfer is enhanced. On the contrary, at low gravity, where the relative velocity between liquid and vapor is reduced, heat transfer coefficient is lower, due to the absence of induced turbulences at the bubble tails.
- Flow pattern definition cannot be directly linked to the thermal heat flux because there are many parameters that influences the process, such as pressure. For this reason, it is difficult to state with a world wide agreement, the upper limit of the heat flux to avoid thermal crisis because it is strongly dependent on the studied system.

## 8. References

- [1] Shizuo SAITOH, Hirofumi DAIGUJI e Eiji HIHARA, «Effect of tube diameter on boiling heat transfer of R-134a in horizontal small diameter tube,» *International Journal of Heat and Mass Transfer*, n. 50, pp. 5215-5225, 2005.
- [2] Sébastien LUCIANI, David BRUTIN, Christophe LE NILIOT, Lounes TADRIST e Omar RAHLI, «Boiling heat transfer in a vertical microchannel: local estimation during flow boiling with a non-intrusive method,» *Multiphase Science and Technology*, 2009.
- [3] Chiara BALDASSARI e Marco MARENCO, «Review Flow boiling in microchannels and microgravity,» *Progress in Energy and Combustion Science*, 2012.
- [4] Xiande FANG, Da TANG, Ling ZHENG, Guohua LI e Yuliang YUAN, «Experimental investigation of gravity and channel size effects on flow boiling heat transfer under hypergravity,» *Aerospace Science and Technology*, vol. 94, 2019.
- [5] Christopher KONISHI e Issam MUDAWAR, «Review of flow boiling and critical heat flux in microgravity,» *International Journal of Heat and Mass Transfer*, 2014.
- [6] Daiane M. ICERI, Giuseppe ZUMMO, Luca SARACENO e Gherhardt RIBATSKI, «Convective boiling heat transfer under microgravity and hypergravity conditions,» *International Journal of Heat and Mass Transfer*, vol. 153, 2020.
- [7] John THOME, Lixin CHENG e Gherhardt RIBATSKI, «Two phase flow patterns and maps,» *Applied Mechanics Review*, n. 61, pp. 1-29, 2008.